Chronological modelling of the Chalcolithic settlement layers at Tell Yunatsite, Southern Bulgaria

Yavor Boyadzhiev[1], Kamen Boyadzhiev[1], Lennart Brandtstätter[2], and Raiko Krauß[2]

1 National Archaeological Institute with Museum, Bulgarian Academy of Sciences, Sofia, BG
yavordb@abv.bg; kamen.boyadzhiev@naim.bg
2 Institute of Prehistory, Early History and Medieval Archaeology, Tübingen University, Tübingen, DE
lennart.brandtstaetter@uni-tuebingen.de; raiko.krauss@uni-tuebingen.de

ABSTRACT – *This article publishes a new series of radiocarbon dates from Tell Yunatsite, Southern Bulgaria. Context-based excavations undertaken over a large surface area, as well as a small test trench, provided a long stratigraphic sequence (11 'building levels') covering a large part of the Chalcolithic period in Thrace (5th millennium BCE). Bayesian statistics and Gaussian Monte Carlo Wiggle Matching were employed to achieve a fine chronology for the multilayered tell. Implications and problems on the application of the calibration curve for the Late and Final Chalcolithic in Bulgaria are also discussed.*

KEY WORDS – *radiocarbon dating; chronology; stratigraphy; Chalcolithic; Gaussian Monte Carlo Wiggle Matching; Bayesian statistic*

Kronološko modeliranje halkolitskih naselbinskih plasti na telu Yunatsite, jug Bolgarije

IZVLEČEK – *V članku predstavljamo novo serijo radiokarbonskih datumov s tela Yunatsite v južni Bolgariji.S pomočjo v kontekste usmerjenih velikih izkopnih površin in manjših testnih sond smo prepoznali dolgo startigrafsko sekvenco (11 'gradbenih nivojev'), ki pokriva velik del halkolitskega obdobja v Trakiji (peto tisočletje pred našim štetjem). Za natančno kronologijo večslojnega tela sta bili uporabljeni Bayesova statistika in Gaussovo Monte Carlo usklajevanje krivulje. Poleg tega smo analizirali tudi posledice in probleme uporabe kalibracijske krivulje pri datiranju poznega in končnega halkolitika v Bolgariji.*

KLJUČNE BESEDE – *radiokarbonsko datiranje; kronologija; stratigrafija; halkolitik; Gaussovo Monte Carlo usklajevanje krivulje; Bayesova statistika*

Introduction

Tell Yunatsite (42°13'56"N; 24°15'45"E), also known as Ploskata mogila (the 'Flat mound'), is situated in Southern Bulgaria, in the western part of the Upper Thracian Plain (Fig. 1). The diameter is 110 x 100m at its base and the height is 12m above the modern-day surface. The tell developed on a low terrace on the ancient bank of the Topolnitsa River near to its confluence with the Maritsa River[1]. It is located in a fertile plain bounded by mountains – the Rhodope Mountains to the south, Rila and Ihtimanska Sredna Gora Mountains to the west, and Sashtinska Sredna Gora Mountain to the north (Fig. 2).

The first excavations of the site were carried out by Vasil Mikov in 1939. Systematic archaeological excavations of the tell's eastern section began in 1976

---

1 The course of the Topolnitsa River has changed through time and in the 20th century AD it was rectified with dikes.

and continue into the present (*Mikov 1940; Katincharov* et al. *1995; Tell Yunatsite 2007; Boyadzhiev* et al. *2004; 2009; 2011a; 2011b; Mazanova 2011*). So far, the excavations have yielded evidence of habitation from the 5th millennium BCE until the 6th century AD – including Chalcolithic, Early Bronze Age (EBA), Iron Age and Roman Age occupations, as well as a Medieval cemetery. Long-term habitation was documented in two periods – the Chalcolithic and the Early Bronze Age. Seventeen consecutive building levels from the EBA have been excavated over approx. 40% of the tell's area (Yunatsite Б1-Б16/17[2]).

Stratigraphy of the Chalcolithic layer

This paper focuses on the Chalcolithic sequence. Until 2012 the latest layer from this period (building level BI) was excavated over approx. 40% of the tell's area (Fig. 3). A large series of ¹⁴C dates was obtained from this level (*Tell Yunatsite 2007.232–238; Boyadzhiev 2015; Boyadzhiev, Aslanis 2016; Mathieson* et al. *2018*).

Since 2012 research has concentrated on a smaller area in the central eastern part of the tell, known as Mikov's trench (sq. M-H 3-7), and the adjacent squares to the south (sq. O 4-7, П 4-6) (Fig. 4). The main objective has been to understand the stratigraphy of the Chalcolithic habitation. The first step was aimed at exposing the levels between the latest habitation layer (BI) and the surface reached in 1939 at the bottom of Mikov's trench, thus merging it with the squares to the south. The second step aimed at continuing the excavations in this section, gradually reaching the earliest habitation layer of the tell. A stable sequence up with Mikov's trench was provided by detailed research of the remains of consecutive buildings preserving the stratigraphic order of the habitation layers (Fig. 5).

The excavations indicated a long lifespan of the buildings. Different reconstruction events have been attested, including numerous floor plasters, interior renovations (*e.g.*, moving the oven) and even the reconstruction of walls. Based on a partial excavation of the tell, the separation of distinct 'building levels' is therefore quite challenging. In fact, the term 'building level' is here used only provisionally, as different buildings of the tell may have been built or destroyed at different times, had a different period of use and/or went through different interior reconstruction events.

One of the key problems regarding the interpretation of partially excavated unburnt building structu-

Fig. 1. Location of the Tell Yunatsite in Southeast Europe (from Google Earth).

2 During the large-scale systematic excavations the following labelling of the main layers was accepted (in Cyrillic): *A* Roman and Iron Age; *Б* Early Bronze Age; *B* Chalcolithic.

res is the reliable differentiation between renovations of a house (*i.e.* those which occurred within the lifecycle of a 'building level') and the building of an entirely new house (*i.e.* occurring at the start of a new 'building level'). Similar problems emerge in small excavated areas with no building remains at all (especially with no floor-destructions-floor superpositions) or layers without distinctly identifiable limits.

Since 2000, renovations of a single building at Yunatsite are considered to be part of one 'building level'. A new level, on the other hand, is marked by the entire destruction of a building, as evidenced by a layer of debris covering its surface and/or by a levelling layer separating the remains of one building from those of another. The high probability that neighbouring buildings have different lifespans is also considered. So far (until 2019), six 'building levels' have been identified.

Building level BI

The latest (uppermost) Chalcolithic building level was largely exposed before the year 2000. During these earlier excavations, it was assumed that the base of building level BI was marked by the level of the uppermost floor of the respective buildings (*Matsanova, Mishina 2018*) (Fig. 6). Newer research between 2002 and 2017, however, showed that level BI covered a much longer time-span. Consecutive floor plasters and reconstructions of interior structures (*e.g.*, ovens) were attested, showing earlier stages in the lifecycle of a single building.

Reliable stratigraphic evidence for the superposition of level BI and the lower levels was revealed in two

Fig. 2. Aerial view from the East over the Pazardzhik field with Tell Yunatsite in the centre.

sectors on both sides of Mikov's trench. The first sector in the south (sq. П-О 7-3)[3] provided a connection with structures reached in 1939 at the base of the trench. The building (BIII-1) reached in the western part of this trench (sq. O-H 7-6) was assigned to level BIII.

The second sector is located between the northeast corner of Mikov's trench and the periphery of the tell (sq. Λ3-M3) – a small area which was not excavated in 1939. In the upper part of this sector an oven from Building BI-2 from level BI was excavated. Under this level the remains of consecutive buildings (floor plasters and debris) were exposed. Due to erosion at the edges of the tell the upper layers were more eroded and less preserved compared to the lower features.

Building level BII

In 2001–2003, two buildings from building level BII were uncovered in the northern part of the tell (BII-14 and BII-15). Both were continuously used, with

Fig. 3. Photogrammetric model of Tell Yunatsite with the area studied in 2012–2019 (graphic by B. Whitford).

---

3 The labelling of the squares follows the Cyrillic alphabet.

two major construction phases (*Bo-yadzhiev* et al. *2004. 170*).

The most important structures to clarify the stratigraphy of the Chalcolithic layer were three buildings from level BII excavated in 2014–2019 south of Mikov's trench.

Building BII-22 is situated in the easternmost part of the tell (sq. O3-O4). The western wall was attested, and it is at least 8m long and oriented N/NE – S/SW. In the northern part of the building the base of an oven was uncovered. It is situated under oven No. 1 from building BI-6, level BI (*Matsanova, Mishina 2018. 129, 135–136, Fig. 12.1*). Most of building BII-22 was uncovered under building BI-6. Its debris was levelled when the surface of level BI was prepared for the construction of building BI-6.

Building BII-21 is located west of building BII-22, in squares O4-O5, П4-П6. It is approx. 10.60m long and 8.50m wide and divided into a few separate 'rooms'. An upper floor made of greenish clay was exposed. In some negative structures cutting this floor level a stratigraphic sequence of more floor plasters is visible, testifying the continuous lifecycle of the building.

In the northeast part of the building a podium was found built on top of the greenish clay floor. Under this a lower podium was attested in the profiles of some negative features.

The building burned down in a sudden event. In two of the 'rooms' a high concentration of broken vessels, some filled with charred grains and fruit seeds, were uncovered. On top of the floor and the burnt building debris there was a plaster of fired clay (in some places a sequence of a few plasters), followed by a homogeneous layer of black clayish soil, a layer of grey-greenish soil and a layer of levelled orange debris. In these layers no structures were found (except for small trenches and postholes), and only few finds were recorded. The uppermost layer of debris is covered by the base of level BI.

The analysis of this depositional process connected to the destruction of building BII-21 shows that the fire did not affect (or at least not heavily) the neighbouring building BII-20 (to the west). While the
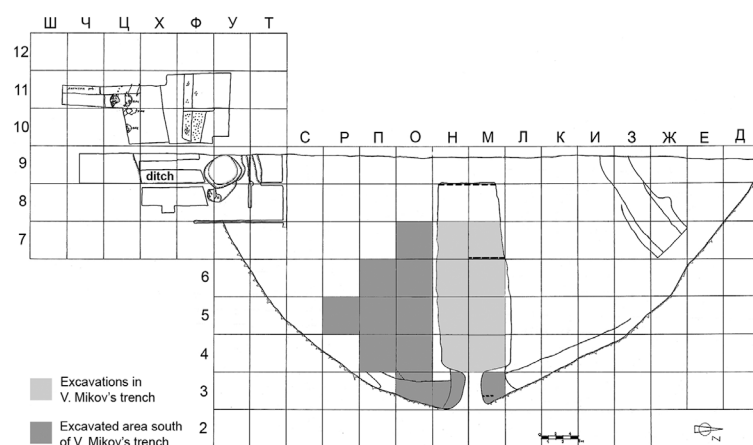
Fig. 4. Tell Yunatsite. General plan of the excavated part of the tell and the area studied in the last years. Locations of the profiles illustrated in the paper are marked with dashed black lines (graphic by Y. Boyanin and K. Boyadzhiev).

above-mentioned homogeneous layers of black and grey-greenish soil accumulated, BII-20 still existed after this event. Building level BII obviously covers a long timespan, with different reconstruction events in different parts of the settlement.

The sample Poz-108890 (5620±40 BP) is a bone (*Bos taurus* phalanx) taken from the layer of grey-greenish clayish soil under the levelled debris (context 222C), in sq. П4. It marks the final phase of level BII in this area.

The sample Poz-109086 (5590±40 BP) was taken from a concentration of charred lentils stored in vessel 10 and found under the burnt debris (context 385), on top of the greenish floor level in the northeastern part of building BII-21 (sq. O4). It dates the burning event.

Building BII-20 is situated west of building BII-21, in squares O6-O7 and П6. It is preserved partially under building BI-8 from level BI (*Matsanova, Mishina 2018.129, 135, Fig. 12.1*) and had at least two construction phases. The bone sample Poz-108910 (*Bos taurus*, phalanx) was taken from the homogeneous clay surface (context 48) underneath the burnt debris which defined the end of the building.

In the small area east of Mikov's trench (sq. Λ3-M3) building level BII is defined by a sequence of 11 floor plasters, preserved over an area of two square metres (*Boyadzhiev* et al. *2015.95–96*).

Building level BIII
One building from this level has been partially excavated – building BIII-1. Its location is essential in cla-
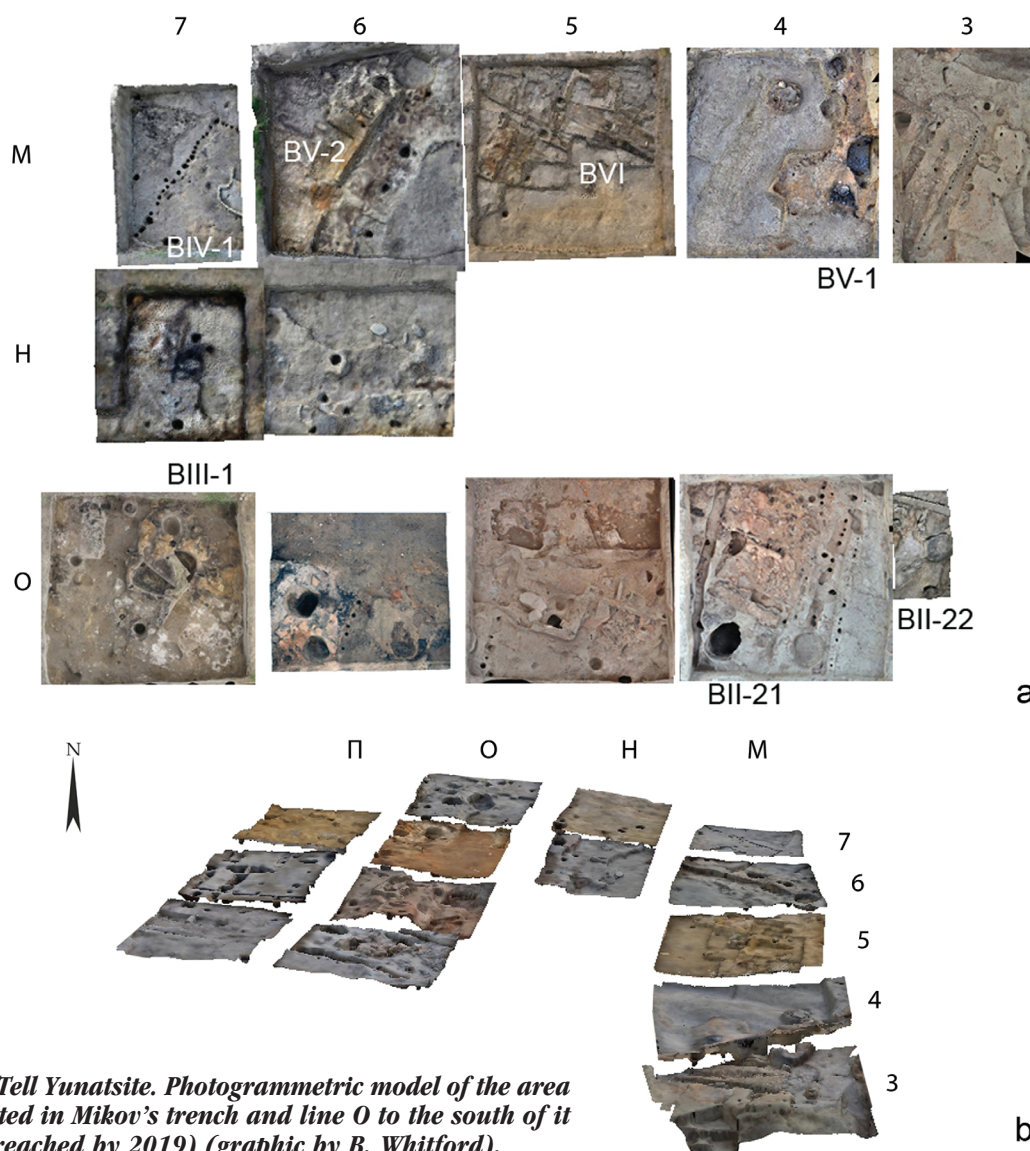
Fig. 5. Tell Yunatsite. Photogrammetric model of the area excavated in Mikov's trench and line O to the south of it (level reached by 2019) (graphic by B. Whitford).

rifying the stratigraphic connection between Mikov's trench from 1939 and the recently excavated area to the south. The southern half of the building was uncovered under the base of building BII-20 (in sq. O6-O7), while its northern half was documented in the western part of Mikov's trench (sq. H6-H7). North of the building, in sq. M7, a concentration of animal bones was found. Under it and the northernmost debris of building BIII-1 a levelling layer of greenish clay was attested (the base of level BIII). It covered the remains of building BIV-1 from level BIV (Fig. 7).

Building BIII-1 consisted of two rooms – a southern and a northern one. Several reconstruction events were documented in both rooms, which were independent of one another. In the northeastern part an oven was found, which was built on sediments on top of the earliest floor level. Later, the oven was abandoned and covered with a thin clay plaster and a wooden construction was installed east of it. The building was destroyed by fire.

Two ^{14}C dating samples were taken. The sample Poz-109084 (5730±40 BP) was taken from a concentration of charred grain found under the burnt debris of the building BIII-1 (context 90) in the southwestern part of the northern room (NW corner of sq. O7). It dates the burning event of the house and the end of level BIII. The bone sample (*Bos taurus* phalanx) Poz-108885 (6130±40 BP) was taken from an earlier layer of the building – context 278 in sq. H6. Compared to the other dates from the site, it is clearly too old for the layer and was excluded from the analysis.

In the area east of Mikov's trench (sq. Λ3-M3) the remains of a building with six consecutive floor plas-
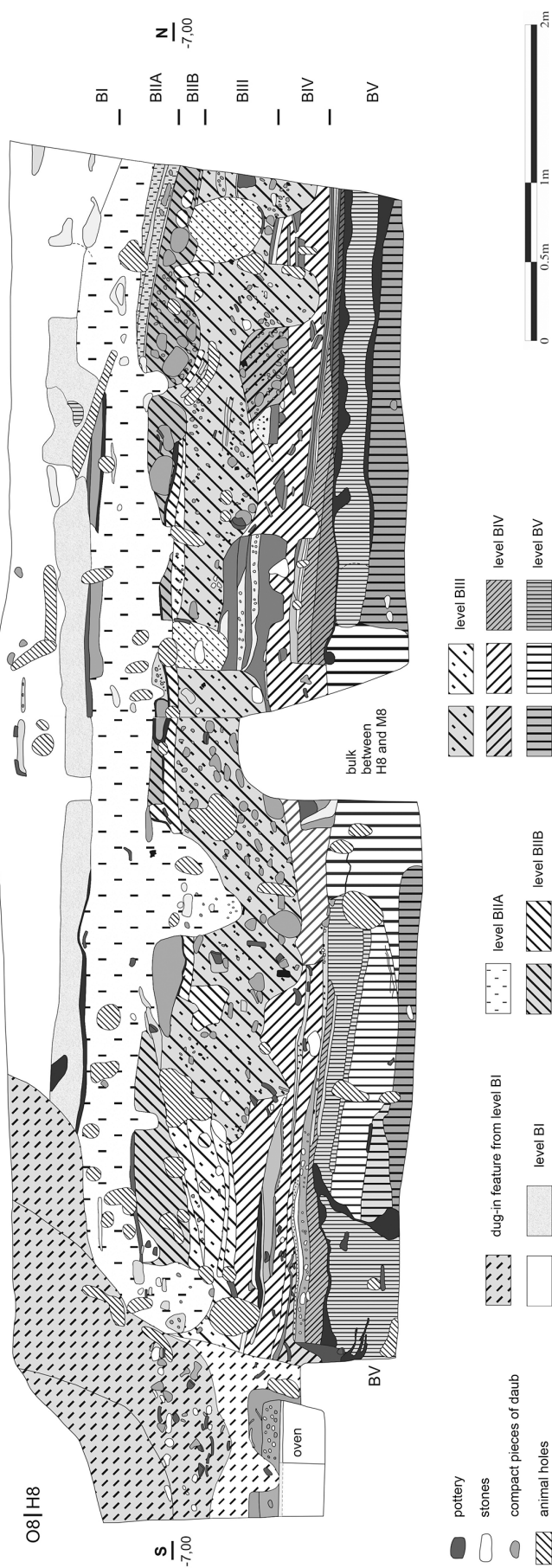
256

Fig. 6. Tell Yunatsite. West profile of Mikov's trench, sq. M8-H8 (graphic by K. Boyadzhiev).

ters belong to building level BIII. The remains of a base of an oven or fireplace were found (*Boyadzhiev* et al. *2015.95–96*).

Building level BIV

Building level BIV has been studied in two small areas, in the western part of Mikov's trench (sq. M7 and partly in M6) and in the small area east of Mikov's trench (sq. Λ3-M3).

In squares M7 and M6 the remains of building BIV-1 have been partially excavated. The southern part of the building is preserved under the northern part of building BIII-1 and is not yet excavated. Its 'western' and 'northern' walls were identified by 0.20m wide ditches. The orientation of the house is NE to SW.

The osteological material from the building is scanty and very fragmented. Two bone samples were selected from the heavy fraction of the flotation of a clayish layer that is located on top of the floor in the southeast part of sq. M7 (Poz-108886 (5630±40 BP [context 230, unidentified long bone]); Poz-115801 (5730±40 BP [context 225, *Ovis/Capra* vertebra])). Both samples were obtained from flotation and should be handled with more care since they were not collected during the excavation of the features.

A small part of another building (BIV-2) was excavated in the eastern periphery of the tell, in squares Λ3-M3. A floor with five consecutive plasters was documented (Fig. 8). The base of the fired eastern wall was found, identified by two rows of mudbricks. The remains of the base of an oven or fireplace was uncovered under the oven/fireplace from building level BIII (*Boyadzhiev* et al. *2015.96; Boyadzhiev, Aslanis 2016.137*).

The bone sample (*Ovis/Capra* femur) Poz-108883 (5710±40 BP) was collected from a concentration of animal bones (context 348) east of the building BIV-2, on top of a layer of green clay marking the very base of building level BIV.

Building level BV

Two buildings from this level were partially excavated: BV-1 and BV-2. Their positions in the stratigraphic sequence are well understood (Fig. 9). Building BV-2 was uncovered under the remains of building BIV-1 in sq. M6-M7. So far, it has been excavated in sq. M6, but is also preserved to the south (sq. H6-H7) and north (outside of Mikov's trench). To the west, its destructions have been documented in the entire sq. M7. The orientation of the building is N/NE-S/SW. It was heavily burnt, which left the osteological material in poor condition. A few samples were collected for dating, but these lacked enough collagen. One bone sample (*Bos taurus* phalanx) from the destruction (context 35E, sq. M6) could be dated: Poz-109419 (5460±50 BP), but had a critically low amount of collagen (0.2%). It is the youngest date in the series of radiocarbon dates and does not fit to the documented position in the stratigraphy of the site. Therefore, it was excluded from further analysis.

Building BV-1 is situated in the eastern periphery of the tell – sq. Λ3-M3-M4. Its remains were covered by the floor of building BIV-2 and the green clay layer mentioned above. At the base of the floor, constructed using an atypical construction technique that consists of tightly placing clay lumps close to each other, two construction phases were detected. During the second phase, the oven was rebuilt in the northeast part of the building and slightly shifted in its orientation. The base of clay lumps was carefully plastered with clay to build a flat and steady floor surface. Three more 'packages' of clay plasters were preserved above this floor, testifying three more reconstruction phases. Reconstruction phases were also documented by the re-plastering of the oven and by a slight shift of the eastern wall. These reconstructions indicate a long lifespan of the building.

The bone sample (*Bos taurus* phalanx) Poz-115802 (5700±40 BP) was taken from a layer on top of the latest floor (context 396), but under the debris of the building BV-1, and it marks the final phase of the building. Chronologically its position is closer to the beginning of the building level BIV (samples Poz-108886; Poz-108883; Poz-115801), than to the beginning of level BV.

Building level BVI

This building level was preserved in the easternmost periphery of the tell. A very small part of a building BVI-1 was excavated. It was partly covered by the floor of building BV-1. The eastern part at the edge of the tell was eroded. A sequence of 14 floor plasters from BVI-1 was uncovered and was found tilting to the south and west. A few bones, including sample (*Ovis/Capra* metacarpus) Poz-108907 (5630±40 BP), were found lying on the uppermost plaster (context 439).

Building level BVI was also attested in sq. M5, in the area between buildings BV-1 and BV-2 (Fig. 5). Four ovens with a concentration of white ash surrounding them were found in this sector just below the level reached by Mikov in 1939. The two earlier ovens have been built on platforms made of wooden beams, which were preserved unburned. Stratigraphic observations of the buildings BV-1 to the east and BV-2 to the west indicate that these ovens belong to the earlier building level (BVI), while the two later ovens are probably synchronous with the buildings from level BV. Possibly this open area between the houses was used continuously during the time of the building levels BV and BVI. Similar situations were attested in levels BI and BII as concerns the space between buildings.

The bone sample (ungulate, vertebra) Poz-115803 (5690±40 BP) was collected from a clay layer (context 118) on top of the unburnt wooden platform and is most likely related to building level BVI.
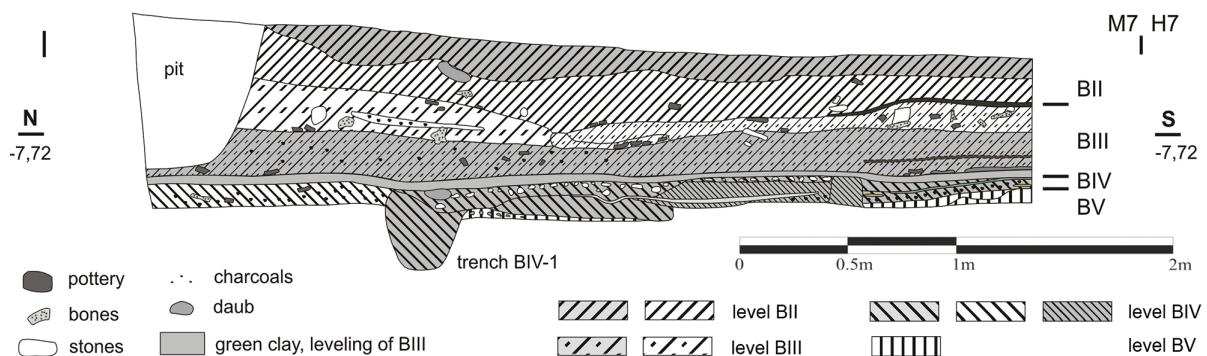

Fig. 7. Tell Yunatsite. Sq. M7, east profile (graphic by K. Boyadzhiev).

Building level BVII

To obtain additional stratigraphic information and collect samples for ^{14}C dating, a small test-trench was dug in the eastern periphery of the tell (sq. M2-M3 – Figs. 4, 8). It measured 1.30 (N-S) x 0.80m (about 1.04m^2) in the upper part and was narrowed to 0.80 x 0.30m below the depth of –8.76m. It cut the preserved parts of the layers below BVI which did not erode. The trench is stratigraphically related to the floor of building BVI-1. Under this floor a compact layer of burnt debris was exposed. About 0.40m below the debris a hard-plastered floor was found. It probably marked the lowest (earliest) floor of the building, whose destruction material was attested above. Two more probable floors were exposed 0.12m and 0.25m above the earliest floor, but under the debris. Two spots of burned clay with a diameter of about 0.50m were stratigraphically related to these floor levels. The lower one was 1.5cm thick and the upper one was 2.5cm thick.

Although the excavated area is very small, the stratigraphic observations indicate that these layers belong to one building with three occupational phases. Bone sample (*Dama dama* tibia) Poz-108905 (5680± 30 BP) is taken from a greenish grey layer (context 450) related to the second phase.

Building level BVIII

No remains of floors or burnt debris were excavated underneath building level BVII. Several layers with different characteristics were identified and separated into probable 'walking surfaces': trampled clay levels with horizontal concentrations of pottery sherds and other artefacts. They might mark different building levels, but the very small area of the test-trench does not provide grounds for reliable conclusions. Thus, these levels were arbitrarily labelled as BVIIIa, BVIIIb, BVIIIc and BVIIId (Fig. 10).

Level BVIIIa

The base of this level is marked by a thin layer of burned clay. A few pottery sherds and some animal bones (including sample Poz-108908 (5740±

Fig. 8. Tell Yunatsite. East profile of the Mikov's trench, sq. Λ4-M4 (photo by Y. Boyadzhiev).

40 BP) [*Bos taurus* costa]) were found in a grey ashy layer (context 474) on top of it. A 0.30 to 0.40m thick layer of grey-greenish soil with small pieces of daub and a lot of charcoal covered it.

Level BVIIIb

This level was approx. 0.40–0.50m thick. Its upper part is marked by a layer of grey-brown ashy soil, up to 0.25m thick to the south and thinning to the north. In the southern part of the test-trench two thin layers of yellow clay were exposed below it, and a thin layer of white ash on top of it. A very tiny level of dark soil separates the clay layers. A greenish-grey sandy layer was exposed under these layers and at its base a structure of unburnt wooden planks

Fig. 9. Tell Yunatsite. Sq. M2-M3-Λ3: building BV-1 (level BV) and the location of the test trench in the periphery of the tell to the east of it (photo by K. Boyadzhiev).

was revealed. Four parallel horizontal planks were uncovered, which were oriented NW to SE. They were 8–10cm wide, more than 0.80m long and are still preserved in the western profile. The distance between the planks was 5–10cm. Underneath them a second layer of perpendicular planks (SW to NE) was recorded. 0.15m above the northern end of this feature, pieces of unburnt wooden planks oriented NW-SE were uncovered, as well as a preserved plank with the same orientation above them. They were divided by a thin layer of grey-greenish sandy soil (context 505). The bone sample (*Bos taurus* humerus) Poz-108906 (5810±40 BP) was taken from this place. North of these planks a vertical, 0.13m wide plank was found, placed on its longitudinal side. All wooden planks were found in or slightly below the greenish grey sandy layer.

In the northern part of the test-trench the grey-brown ashy layer was much thinner. A thick layer of grey-brown clayish and sandy soil was exposed below it (context 484). A few pieces of a broken oven or fireplace were documented inside it. In the upper part of this layer the concentration of pottery sherds was higher and the bone sample (*Bos taurus* humerus) Poz-108888 (5780±40 BP) was taken from there. It possibly marks a later 'phase' of level BVIIIb compared to Poz-108906 (5810±40 BP).

Level BVIIIc

After the documentation of the wooden construction, the research in the southern part of the test-trench was stopped to preserve the structure *in situ* and study it in the future over a larger area. Excavations continued in the northern part, covering an area of 0.80m (N-S) by 0.30m (E-W). A level of –10.72m below the highest point of the tell was reached, 0.90m below the elevation of the unburnt wooden planks. Seven layers were identified in these 0.90m. Some contained tiny layers of white ash. The overall thickness of these layers and their number indicated that they were related to at least two building levels. The upper one is marked as BVIIIc and is about 0.55–0.60m thick. A layer of hard fired clay (floor plaster?) probably marks its base.

Sample Poz-108889 (5810±40 BP [*Bos taurus* costa, hard grey clay, context 518]) was taken from a grey layer on top of this base.

Level BVIIId

The lowest level is about 0.30–0.35m thick. Three layers separated by thin layers of ash were identified. Bone sample (*Bos taurus* metacarpus) Poz-108909 (5860±40 BP) was collected from the uppermost (grey soil with some charcoal – context 521) of these layers. A second bone sample (*Bos taurus* costa) Poz-108887 (6200±40 BP) of level BVIIId has been taken from an ashy grey layer (context 523). The calibrated date is the oldest radiocarbon date from the site, comparable with the sample Poz-108885. It is obviously too old for the dated layer and therefore has been excluded from further analyses.
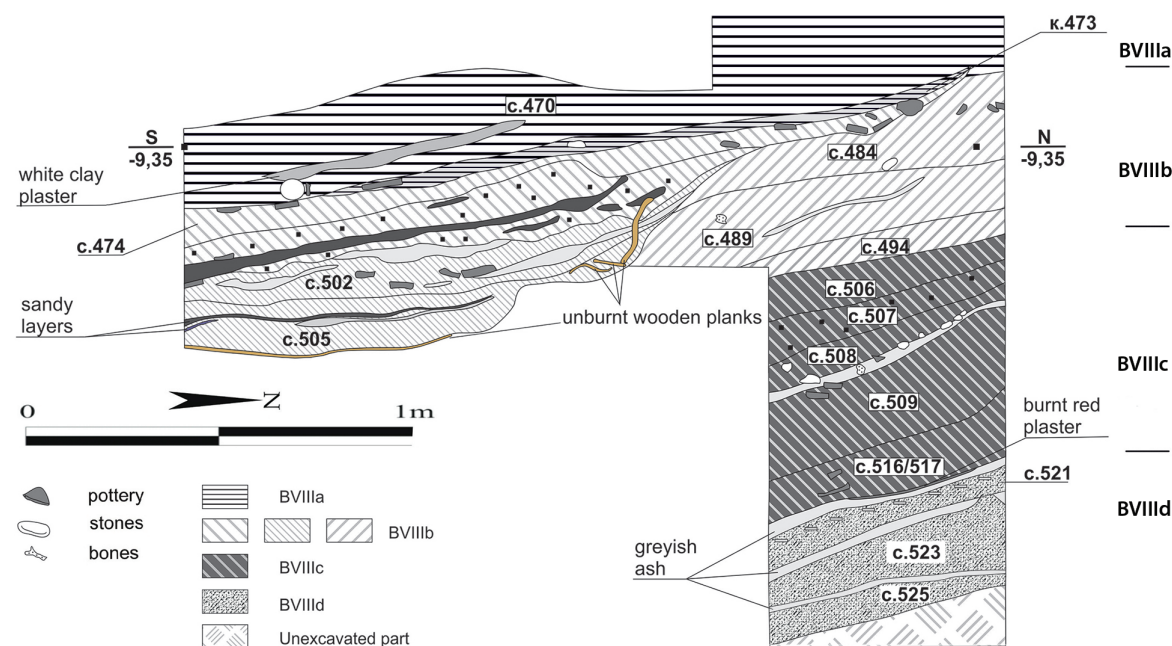

Fig. 10. Tell Yunatsite. Sq. M2-M3: profile of the test trench in the eastern periphery of the tell (graphic by S. Ivanov).

The highest point of the Chalcolithic layer in this part of the tell is defined by the burnt debris of building BI-2 from level BI (in sq. Λ-K/5-4) and was measured at –5.25/–5.35m (below the highest point of the tell). The lowest depth reached in the test-trench is –10.72m, proving a thickness of at least 5.20m for the Chalcolithic layers. The sterile soil has not been reached and at least 11 building levels were identified.

Relative chronology of the Chalcolithic building levels

The main material to build up a relative chronology of the Chalcolithic building levels is ceramic. Unfortunately, the assemblage of the levels below BV is very scanty, as they have been excavated over a very small area. In the analysis of the pottery style of Yunatsite, a general conservatism can be observed resulting in the long, continuous existence of distinct shapes, decoration styles and motifs.

Building levels BVIIId – BVI
The ceramic assemblage from levels BVIIId-BVI is too scanty for detailed analysis and conclusions. It may be generally related to the Early Chalcolithic, Maritsa culture. Only the pottery associated with the platform of unburnt wooden planks and ovens in sq. M5, which was stratigraphically assigned to level BVI, was more numerous. It carries some typical features of phase III of the Maritsa culture.

Building level BV
The assemblage from level BV fits well with the characteristics of phase III of the Maritsa culture (*i.e.* the end of the Early Chalcolithic), as defined by Henrieta Todorova (*1986.101*). Among the typical shapes are dishes with slightly inward-curved rims and graphite decoration on both sides, S-shaped dishes and bowls and lily-shaped dishes. The latter two types are usually painted with graphite on both sides. Dishes with incisions on the rim have also been found. Bowls and jars are predominantly represented with rounded shapes. The common decoration techniques are graphite painting (usually covering large parts of the vessels or even their entire surface) and incised decoration. The so-called 'ladder-like' incised ornament is attested.

Building level BIV
The pottery from level BIV is quite scanty (less numerous than the collection from BV), and few shapes could be distinguished reliably. In general, the assemblage shares many of the typical characteristics

of level BV. Simple conical dishes and dishes with inward-curved rims dominate. The latter are usually decorated with graphite on both sides. Bowls and jars are predominantly preserved with rounded shapes, sometimes with abundant graphite decoration. Fragments of three-partite bowls with an outlined middle part were also attested, and their upper part is decorated with graphite. This shape developed further in the Late Chalcolithic. A few sherds of jugs with vertical handles and graphite paint were found. One fragment of a jug with a horizontal handle on the neck is documented. Among the decorated fragments, graphite paint dominates. It seems that it covered a large part of the vessels and both sides of dishes and bowls. Incised decoration is less frequent and usually found on sherds of storage vessels.

The specifics of this assemblage suggest its dating to the transition from the Early to Late Chalcolithic, or to the so-called Middle Chalcolithic (phase IV of the Maritsa culture).

The most interesting find from level BIV is a small golden bead. It can be related to the earliest golden artifacts known worldwide – beads from the burials of Varna II and the cemetery of Durankulak (*Todorova, Vaisov 2001.13*). They are assigned to the Middle Chalcolithic as well.

Building level BIII
The ceramic assemblage from level BIII (mainly building BIII-1) shows continuity with the pottery from the lower levels. Some typical characteristics from levels BIV and BV are still present in the collection: dishes with inward-curved rims and rounded bowls, rich graphite decoration, incised decoration, as well as most of the motifs. New shapes that are considered typical for the Late Chalcolithic appear: biconical bowls with carination, dishes with an inverted rim or with an inward thickened rim. Shell impressions are also attested.

Additionally, a few flat bone figurines were found in building BIII-1 (*Boyadzhiev* et al. *2017.112, obr. 2*). In general, the earliest known figurines of this kind appeared in the Middle Chalcolithic, but their large-scale distribution is assigned to the Late Chalcolithic (*Boyadzhiev 2007.89–91*).

Building level BII
The pottery assemblage of level BII resembles the characteristics of a 'developed' Late Chalcolithic or phase II of the Karanovo VI horizon. Biconical bowls are more abundant. New shapes appeared and de-

veloped in level BI: 'elaborate' bowls and amphora-like vessels. Shell impressions are used more widely. Graphite painting was still the most common decoration technique and covered a large part of the vessels and the inner surfaces of some types of dishes. In the case of bowls, the decoration is now reduced only to their upper surface.

A golden 'ring-shaped idol' was found in building BII-21.

Building level BI

The ceramic assemblage from the last Chalcolithic habitation layer at Tell Yunatsite includes a large number of complete or restored vessels, which have already been published (*Mazanova 1992; Todorova, Mazanova 2000; Todorova 2003*). The specific characteristics of this complex include new forms, such as biconical cups with two vertical handles and new decoration techniques, such as the use of red[4] and yellow paste or high percentages of positive graphite decoration, which find analogies in the Krivodol culture and indicate contacts to the west (*Mazanova 1992; Todorova, Mazanova 2000.338–341; Todorova 2003.307*).

More than 20 copper artifacts have been found, including two hammer-axes of the Pločnik type (*Mazanova 2004*; new finds from the recent excavations).

Building level BI is dated to the final phase (III) of the Karanovo VI culture. It was destroyed by an enemy attack, the inhabitants were killed, and the buildings were burnt down.

After this event, the tell was abandoned for at least 1000 years. During this long period a hiatus layer accumulated. Due to a tilt of the surface to the south as well as the remains of the Chalcolithic fortification wall, which stopped the erosion of the sediment, this layer is best attested in the southern periphery of the tell, where it is up to 0.40m thick.

Modelling of the radiocarbon dates

To achieve greater precision compared to single measurements, the available stratigraphic information was employed to model the new set of radiocarbon dates. These models were analysed using 'Gaussian Monte Carlo Wiggle Matching' (GMCWM) and Bayesian Sequencing. Both approaches were performed, analysed and compared.

Selection of the radiocarbon samples

The material for radiocarbon measurements was carefully selected in 2018 from reliable contexts excavated between 2014 and 2018 (Tab. 2, see Appendix). The material from building levels BII to BVI was excavated by context over a large surface area. Material from BVII to BVIIId was selected from the small test-trench in sq. M2-M3, where the depositional processes were harder to observe. Samples visibly affected by bioturbation were excluded. Only short-lived plant material and animal bones were considered suitable for measurements. The species of the bone samples were determined, and where possible bones from herbivores were chosen. In some rare cases a determination was not possible or omnivores, mostly pigs, had to be picked.

The quality of the samples from different building levels varied enormously. No new measurements have been made for level BI, since there are already reliable dates available from short-lived materials (Tab. 1, see Appendix) (*Boyadzhiev, Aslanis 2016; Mathieson* et al. *2018*). Three samples from human bones and teeth (Ly-5999/SacA-15568, MAMS-28134, MAMS-28135), as well as one sample from charred grain (Ly-5997/SacA-15566), were included. There are some charcoal samples from BI that fit well with the other samples, but they were excluded from the analysis to reduce further uncertainty, especially since these samples define the end of the Chalcolithic habitation at the site.

The samples from level BII seem to be reliable and fit well between BI and BIII. They include samples made of charred lentils (Poz-109086) and cattle bones (Poz-108890; Poz-108910).

There is only one sample (Poz-109084) from level BIII. It was measured from charred grain found in the destruction of house BIII-1. Even if the unmodelled date seems rather late, it should be considered as reliable given the clear context and material. Due to the character of the highly burned debris of the houses from level BIII, no collagen could be extracted from any other bone sample.

The sample Poz-108883 was taken from a concentration of bones covering building BV-1. Since there were no other bones from reliable contexts from the wider excavations recorded, the samples Poz-108886 and Poz-115801 were measured from animal bones taken from the heavy fraction of the flotation of a

---

4 However, the use of red paint is attested in the lower levels as well.

floor layer covering the house BIV-2. These samples are less reliable.

The sample Poz-115802 was found under the debris of building BV-1 and is the only sample from level BV. The debris of buildings BV-1 and BV-2 was heavily burned and no collagen could be extracted for further measurements. Compared with the age of the samples Poz-109084 (debris of BIII-1) and Poz-108883 (reliable context covering BV-1) the unmodelled date might seem too young. In the future further measurements should be done for this building level.

The sample Poz-115803 was collected from a layer covering the wooden planks assigned to level BVI. This area was left open in the building levels BV and BVI and the sample was assigned to level BVI. A second sample Poz-108907 was taken from a concentration of bones covering the uppermost plaster of a sequence of 14 plasters belonging to the building BVI-1, which was partly covered by a floor of the building BV-1.

The samples from the levels BVII to BVIIId were obtained from the small test-trench in squares M2/M3. The size of the trench was about 1m², which made observations limited. Samples were taken from layers that were interpreted as floors. Further excavations over a larger surface area will clarify these preliminary observations.

Gaussian Monte Carlo Wiggle Matching (GMCWM)

The methodology of wiggle matching was first applied by Charles W. Ferguson, Bruno Huber and Hans E. Suess (*1966*). Gordon W. Pearson (*1986*) described it first in mathematical detail, while Bernhard Weninger (*1986*) used it for sequenced archaeological data. A detailed comparison of wiggle matching methods was published by Christopher Bronk Ramsey *et al.* (*2001*). The GMCWM approach used in this article is an extension to the Wiggle Matching method and was outlined by Weninger (1997) and Reinhard Jung (*Weninger, Jung 2009*) to refine the method and widen its possible use. It is integrated in the program CalPal (*Weninger, Jöris 2008*).

In principle the method is using χ^2-tests to match the best-fit between two datasets (the calibration curve data and the archaeological test sample) performing an optional number of runs. To achieve this, an equidistant model, a model with fixed distances between the samples, is needed. The method was specially designed for archaeological applications and is explained in detail by Weninger (*Horejs, Weninger 2016.135*). The aim of this approach is to identify the overall best-fitting archaeological timespan for the series of radiocarbon dates.

The technical parameters for each model used in this study were the same. Each Wiggle Matching run was performed 1000 times, each time only storing the result of the best fit of 50 replications, where phase-internal changes of the position of the single radiocarbon dates were allowed. Offsets of the calibration curve and a measurement error of the BP-date were included in the modelling by applying Gaussian variability of ±10 years for both parameters. The data fitting was performed using the 'non central Chi-squared' method, described in (*Krauß* et al. *2017.294*). All age-calibrations and analyses employed the presently recommended IntCal20 data (*Reimer* et al. *2020*).

GMCWM model 01

All Chalcolithic contexts exposed by the end of 2018 were grouped into 11 phases (BI–BVII; BVIIIa–d) according to their stratigraphic position and assigned building level. The 16 new ¹⁴C-samples were assigned to these

Lab Code	BP date	Phase	unmodelled date cal BC (2σ)	modelled date cal BC
Ly-5997/SacA-15566	5560 ± 30	I	4399 ± 53	4395 ± 19
Ly-5999/SacA-15568	5560 ± 45	I	4415 ± 79	4403 ± 18
MAMS-28135	5578 ± 23	I	4403 ± 49	4411 ± 16
MAMS-28134	5632 ± 24	I	4452 ± 85	4419 ± 15
Poz-109086	5590 ± 40	II	4423 ± 76	4427 ± 13
Poz-108890	5620 ± 40	II	4448 ± 89	4438 ± 12
Poz-108910	5660 ± 40	II	4485 ± 119	4449 ± 10
Poz-109084	5730 ± 40	III	4573 ± 115	4460 ± 8
Poz-115801	5730 ± 40	IV	4573 ± 115	4492 ± 4
Poz-108886	5630 ± 40	IV	4451 ± 90	4502 ± 4
Poz-108883	5710 ± 40	IV	4566 ± 113	4513 ± 4
Poz-115802	5700 ± 40	V	4564 ± 115	4524 ± 6
Poz-108907	5630 ± 40	VI	4451 ± 90	4556 ± 10
Poz-115803	5690 ± 40	VI	4542 ± 135	4572 ± 13
Poz-108905	5680 ± 30	VII	4527 ± 80	4588 ± 15
Poz-108908	5740 ± 40	VIIIa	4581 ± 120	4620 ± 21
Poz-108888	5780 ± 40	VIIIb	4614 ± 109	4652 ± 27
Poz-108906	5810 ± 40	VIIIc	4665 ± 118	4684 ± 32
Poz-108889	5810 ± 40	VIIIc	4665 ± 118	4700 ± 35
Poz-108909	5860 ± 40	VIIId	4723 ± 113	4716 ± 38

Tab. 3. Results of the GMCWM model 01 for the Chalcolithic layers of Tell Yunatsite.

phases. Additionally, four samples from short-lived material (Ly-5997/SacA-15566, Ly-5999/SacA-15568, MAMS-28134, MAMS-28135) from the uppermost building level (BI) were integrated in the models (*Boyadzhiev, Aslanis 2016; Mathieson* et al. *2018*). For statistical analyses, an equidistant model was used, which assumed phases with an equidistant length independent from the thickness of the layers or the recorded absolute depth of the sample. The levels BI-BVII and BVIIIa-BVIIId were treated equally and it was assumed that they cover the same duration of time. Based on the hypothesis of 11 equidistant phases, GMCWM was performed. Three dates were sorted out according to low collagen (Poz-109419) or because they were obviously too old and dislocated (Poz-108885, Poz-108887).

Based on these assumptions the analysis was performed (Fig. 11, Tab. 3). The 11 phases cover the timespan between 4750 and 4375 cal BC, with an approximate duration of 32 years per phase. Espe-

cially at the beginning and the end of the habitation, the dates fit quite well with the calibration curve.

Bayesian Sequence model 01

Bayesian chronological modelling (*Buck* et al. *1996*) has become a standard tool for analysing radiocarbon samples from archaeological sequences (*Bayliss 2009; 2015; Hamilton, Krus 2018*). The Bayesian chronological model was calculated using the program OxCal, version 4.4 (*Bronk Ramsey 2009a*) and the integrated IntCal20 calibration curve (*Reimer* et al. *2020*).

The same assumptions used for GMCWM model 01 were applied to the Bayesian sequence model (Fig. 12). The 20 radiocarbon dates were grouped into 11 phases and separated by boundaries. Some of the building levels had been exposed to fire and therefore some bone samples containing lower amounts of collagen had to be included. Samples below 1% of collagen have been omitted (Poz-109419). To accom-
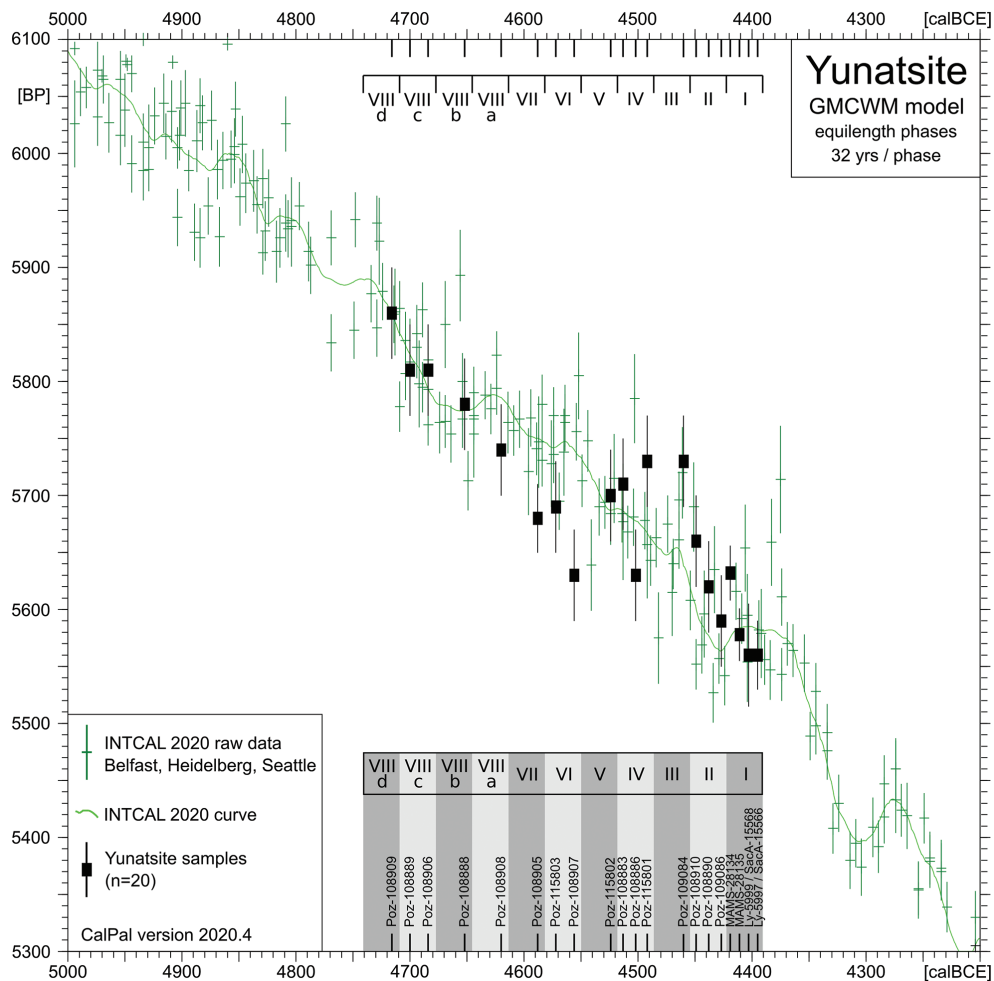

***Fig. 11.** GMCWM model 01 for the Chalcolithic layers of Tell Yunatsite (Gaussian Monte Carlo Wiggle Matching, using the program CalPal 2020.4 (Weninger, Jöris 2008) on the IntCal20 calibration curve (Reimer et al. 2020).*

modate the different amounts of collagen and therefore the different reliability of the sample an r-type Outlier model has been included in the sequence (*Bronk Ramsey 2009b.1038*). The prior probabilities that bone samples with a lower amount of collagen are misleading were set according to the study from Meadows *et al.* (*2019.1660–1662, Tab. 4*),

which was performed using samples with low collagen preservation, mostly measured in Poznan. Prior probabilities for collagen yield between 1–2% were set to 0.4, for 2–3% collagen to 0.2 and for >3% collagen to 0.1. Prior probabilities were not applied to the samples from short-lived plant remains. The model has an overall agreement of A=93.4,
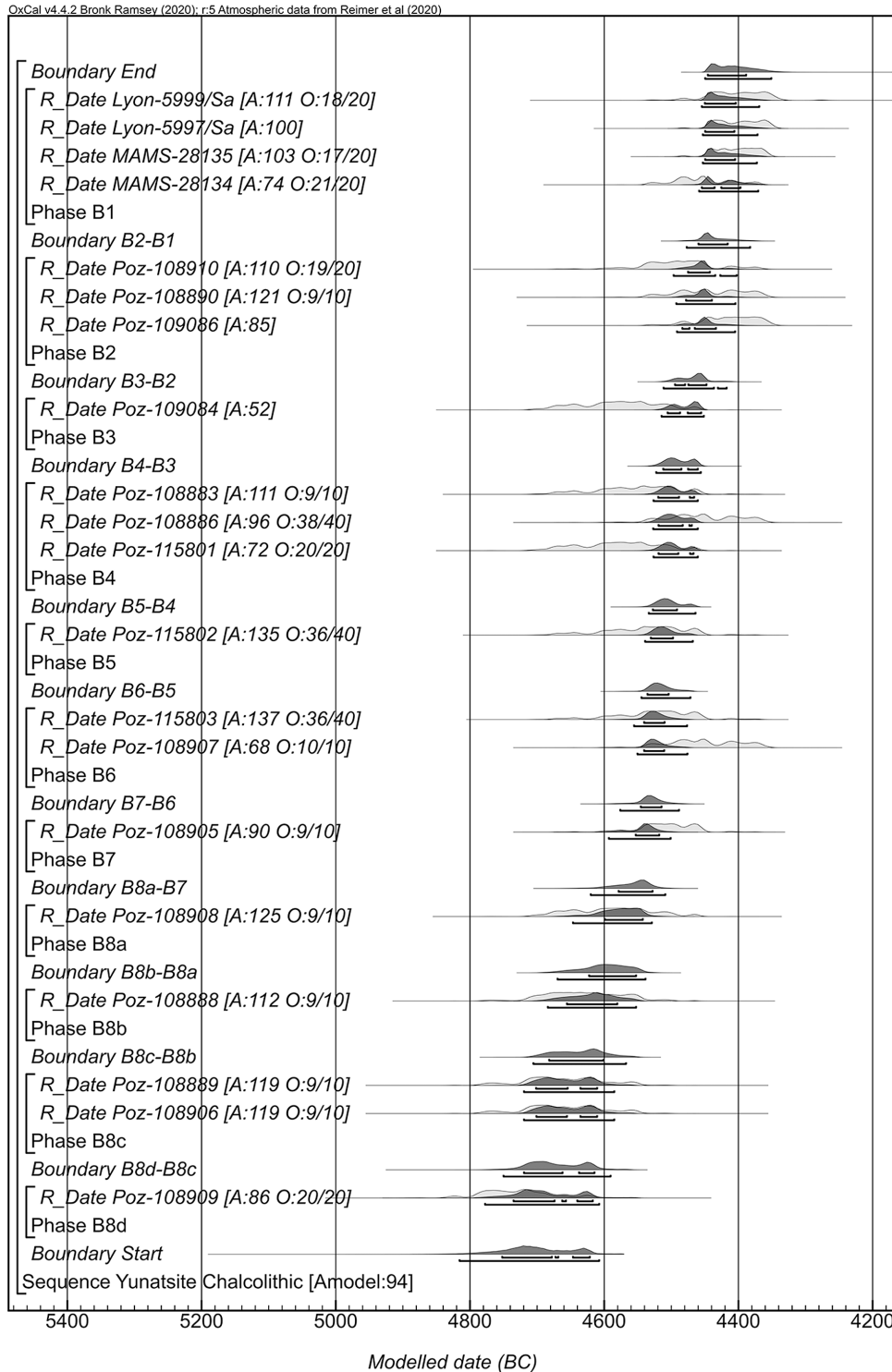

Fig. 12. Bayesian Sequence and Outlier model for the Chalcolithic layers of Tell Yunatsite (using the program Oxcal 4.4 (Bronk Ramsey 2009a) on the IntCal20 calibration curve (Reimer et al. 2020)).

which is robust. Only one probe failed the needed agreement of A=60: Poz-109084 (A=51.5) from building level BIII. This sample was assigned as reliable and the rejection might be caused by possibly relocated or contaminated samples, like Poz-108886 and Poz-108907. Considering the massive cuts und remodelling events at the site, and the layout of the model without any specific filtering or exclusion of radiocarbon dates, the results are good.
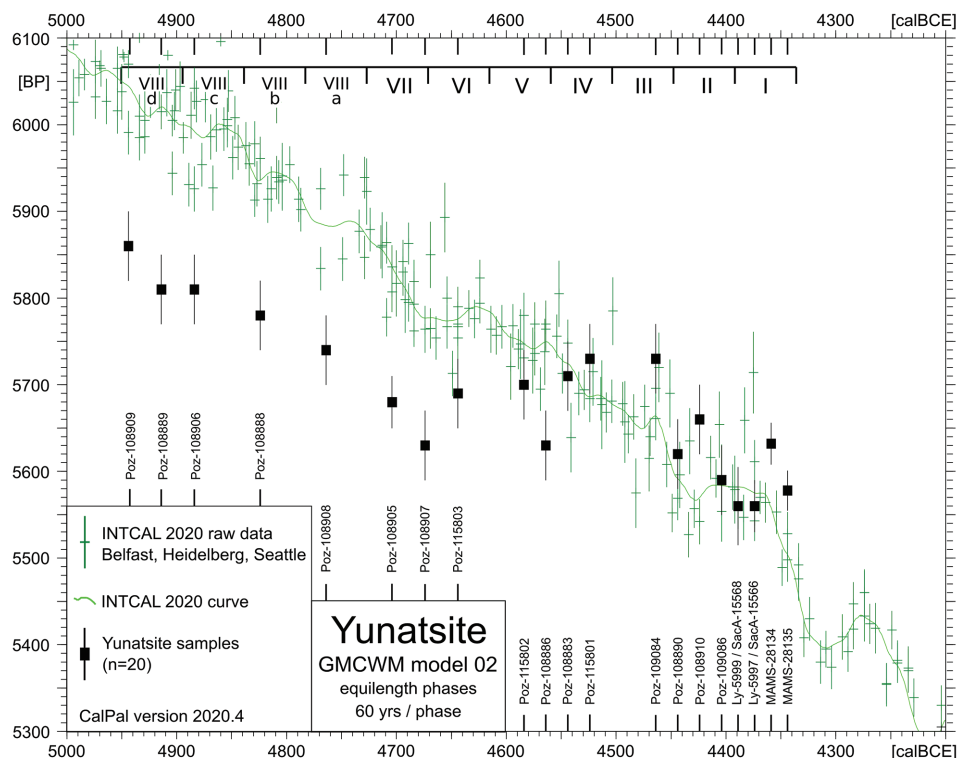
GMCWM model 02

Based on the radiocarbon data from level BVI-BVIIId and typological observations at different Chalcolithic sites in Thrace, one can assume a model with a length of 60 years per phase. This hypothesis (Fig. 13) has been tested by fixing the timespan of every building level to 60 years and modelling it for the best fit. Due to the higher number of dates from layer BI–BIV the model matches best with the younger samples of the data series (level BI–BII), while being unable to match the earlier dates with the calibration curve.

GMCWM model 03

As mentioned before there were problems regarding the low collagen preservation of some bones from burned structures. In particular, building BV-2 and the bones from level BV were affected. Additionally,

the samples from BIV and BVI were less reliable and material of lower quality had to be chosen for dating. This is visible in the longer timespan of the samples from these levels as well as in the summed probability chart (Fig. 14).

To understand the different bias of the series of dates and deal with the problem of the distribution of the samples in the Middle and Late Chalcolithic, an additional model was carried out. The dates were grouped in two different series. The first includes all samples from levels BVI–BVIII(a-d), which refer to the Early Chalcolithic (based on pottery styles). The dates from this period from other tell-sites in Bulgaria correspond well to the calibration curve. The second series with all the samples from the levels BI-BV covers the Middle and Late Chalcolithic sequence. In other sites from these periods in Bulgaria a discrepancy between archaeological data (stratigraphic sequence and relative chronology) and the radiocarbon dates has been observed. The samples in the second series were attained from the excavations in the larger area (squares M-O 5-7), and those in the first were mainly sampled from the small test-trench in squares M2/3. Both series were modelled independently using an approach with equidistant phases. The results were plotted in one graph (Fig. 15.a-b) and compared.

*Fig. 13. GMCWM model 02 for the Chalcolithic layers of the site Yunatsite (Gaussian Monte Carlo Wiggle Matching, using the program CalPal 2020.4 (*Weninger, Jöris 2008*) on the IntCal20 calibration curve (*Reimer et al. 2020*).*
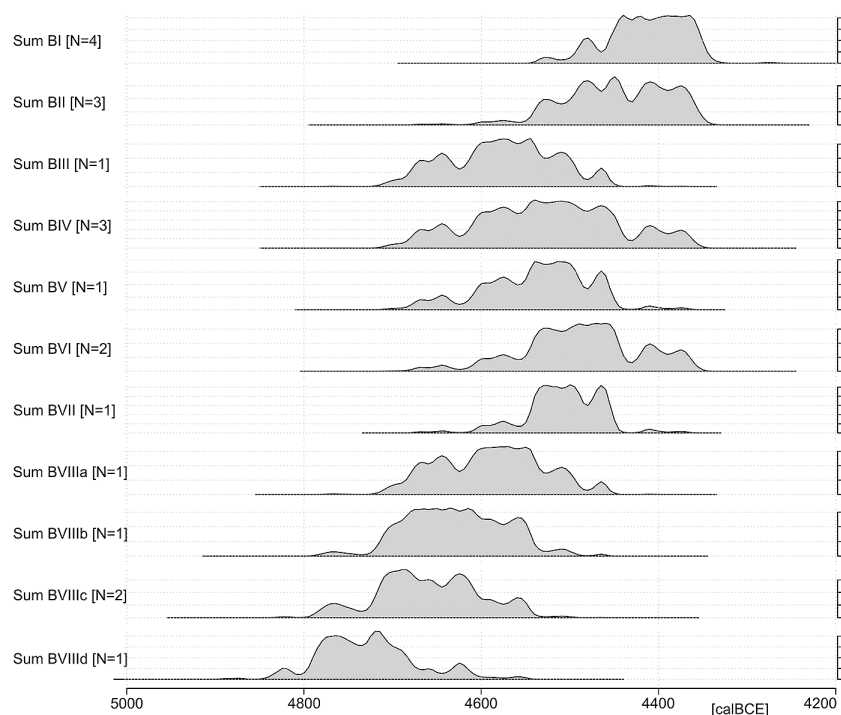
*Fig. 14. Chart of summed probability distributions for each phase (using the package oxcAAR in R (*Hinz **et al.** 2018*; R Core Team 2020*), OxCal 4.4 (*Bronk Ramsey 2009*) on the IntCal20 calibration curve (*Reimer **et al.** 2020*).*

While modelling the set from the levels BVI–BVIIId showed a clear result of 50 years/phase (Fig. 15.a-b – black), the results from the levels BI–BV were blurry and differed in length between 14 years/phase (Model 03a – Fig. 15.a) and 78 years/phase (Model 03b – Fig. 15.b). Both results seemed unreasonable but lack better alternatives. The single radiocarbon measurements used for modelling are located in a plateau of the calibration curve and have standard deviations between 150 and 230 years.

The duration of the two independent models resample the picture from GMCWM model 01, where the samples from levels BI/BII and BVII/VIII mark the beginning and end of the habitation. The samples from the levels in-between are overlaying due to the layout of the calibration curve.

Discussion and conclusions

These models provoke different conclusions and interpretations. Considering the complicated formation of layers at Tell Yunatsite, as well as the challenging preservation, the results are better than expected. While summed distributions for the different levels present unrealistic long durations (Fig. 14), modelling this data strictly according to stratigraphic deposition provides a solid model for the habitation

of the site. Still these results should be treated as preliminary, as future excavations surely will provide more dates, especially for the early levels. Based on the initial assumptions, different chronological trajectories can be made.

Using the current IntCal20 calibration curve, GMCWM model 01 (Fig. 11) would be the best fit. The beginning and end of the series of radiocarbon dates of the Chalcolithic habitation at Tell Yunatsite are at 4750 and 4375 cal BC, respectively. The difficult depositional processes at a tell settlement as well as the general nature of a radiocarbon date are visible in the distribution of the single dates plotted on the calibration curve. Modelling the dates in phases using their stratigraphic information provides a solid way to deal with this data.

This hypothesis was also tested by applying a Bayesian chronological outlier model (Fig. 12) using the stratigraphic sequence. Even without filtering less reliable samples the model agreement is Amodel= 93.4 and solid.

The model suggests an overall chronological duration of 375 years and an average timespan of 32 years/phase (considering 11 building levels or consecutive settlements). These results are in line with published durations of building levels from other tells in the region: Uivar (10–50 years/phase) (*Draşovean* et al. *2017.643, Fig. 7*), Vinča (from a few up to 50 years/phase) (*Tasić* et al. *2016.823, Fig. 14*), Pietrele (40–50 years/phase) (*Reingruber, Rassamakin 2016.281, Fig. 5*), Okolište (30 years/phase) (*Hofmann 2013.473*) or Karanovo (35–40 years/phase) (*Reingruber, Thissen online*). However, such a timespan can be viewed as too short considering some archaeological data from Yunatsite and other Chalcolithic tell-sites in Bulgaria.

First, the correlation of ^{14}C dates series from Early Neolithic multilayered sites with the calibration curve shows average timespans for Early Neolithic building levels (settlements) of about 60–70 years
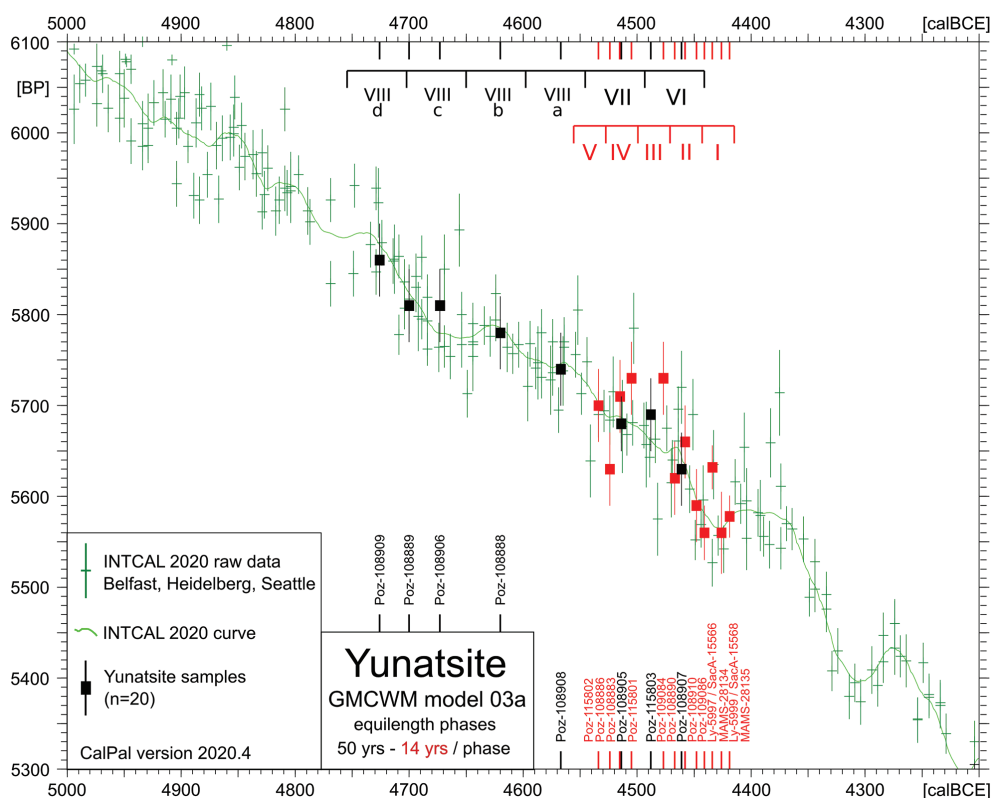
Yunatsite GMCWM model 03a
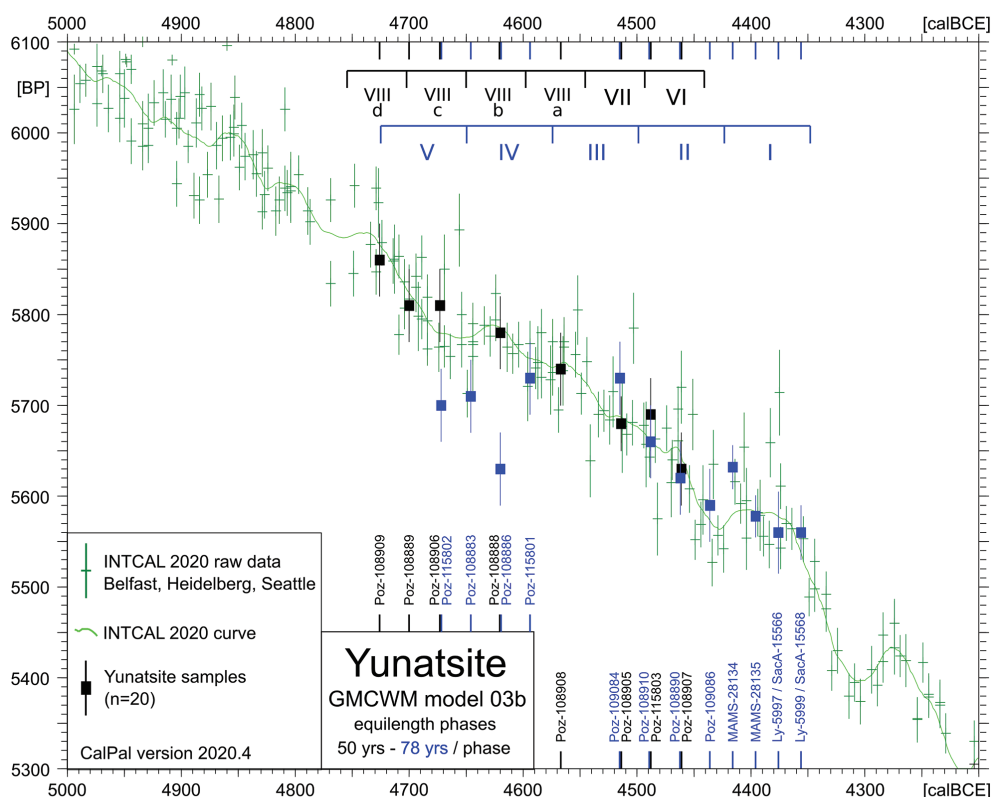
Yunatsite GMCWM model 03b

Fig. 15. GMCWM model 03a/b for the Chalcolithic layers of Tell Yunatsite (Gaussian Monte Carlo Wiggle Matching using the program CalPal 2020.4 (Weninger, Jöris 2008) on the IntCal20 calibration curve (Reimer et al. 2020).

(*Boyadzhiev 1995; Gösdorf, Weninger 1992*). The construction of the buildings, as well as the average thickness of the building's levels, are similar or identical in the Neolithic and Chalcolithic times. We may thus assume that the average timespan of a Neolithic building level was similar to that of a Chalcolithic one.

Second, if we accept this chronological frame for the Chalcolithic levels at Tell Yunatsite we face a large disproportion between the duration of the entire Late Chalcolithic (about 100–120 years, similar situation is attested in Thrace and Northeast Bulgaria) and the final phase of the Chalcolithic. The latter is represented by a small number of thin-layered (one or two building levels) settlements, mainly in Western Bulgaria and the Rhodope mountains. In such a scenario these sites would cover a period of 600 years (4400/4350–3800/ 3750 cal BC; *Boyadzhiev 2015*).

Another option would be to question the layout of the current calibration curve for the period between 4600/4550–4100/4000 cal BC in the region, which is archaeologically identified as the Late Chalcolithic in Bulgaria. For this case, the GMCWM model 02 was designed, which tries to find the best fit on the calibration curve and the test data, accepting a duration of 60 years/phase or 660 years of duration. As discussed above, a time-span of 60 years/phase was chosen based on the durations of multi-layered Neolithic settlements.

This model (Fig. 13) shows considerable deviation between the dates from the early building levels (VIIId to VI) and the calibration curve and fit at the end of the Chalcolithic habitation at the site. The result can be explained by the higher number of dates for the younger levels, which ties the whole series to this part of the calibration curve. The obvious deviation between the calibration curve and the earlier Chalcolithic dates must lead to a rejection of this model.

The third model (GMCWM model 03a-b; Fig. 15) consists of two independently modelled data series: the dates from the Early Chalcolithic (levels BVIIIa-d to BVI) and the dates from the end of the Early, the Middle and the Late Chalcolithic (levels BV-BI). The series from the early levels (BVIIId – BVI) fits very well with the calibration curve in the period between 4725 and 4460 cal BC. The dates from levels BV-BII fit to the calibration curve in the period 4550–4420 cal BC (model 3a; Fig. 15.a) or the period 4680–4350

cal BC (model 3b; Fig. 15.b), but largely coincide with the earlier series. Only the samples from the final phase at Yunatsite (level BI) are later than those from BVI. This situation corresponds well to the ^{14}C series from other Chalcolithic tell sites in Bulgaria: the Early Chalcolithic dates fit well with the calibration curve, but 'drop back' towards the end of the period, leading to overlapping dates between the Early and Late Chalcolithic data series (*Boyadzhiev 1988; 1995.167–173, 182–185; Görsdorf, Bojadžiev 1996.144– 152*).

As described by Yavor Boyadzhiev and Ioanis Aslanis (*Boyadzhiev, Aslanis 2016.165*), the deviation of dates from the Middle and Late Chalcolithic in Bulgaria from the calibration curves may possibly be caused by a local anomaly in the concentration of ^{14}C in the atmosphere. The presence of such an anomaly, as well as its territorial and chronological span, may be ascertained (or not) with series of dates from consecutive levels in multilayered sites, covering all stages of the Chalcolithic period, *i.e.* Maritsa I-IV and Karanovo VI in Thrace and synchronous groups in the neighbouring regions. This phenomenon is not fully understood yet and needs more analyses. The sequence from Yunatsite is hopefully viewed as a reason to intensify this research.

The results from the models draw very different conclusions for the absolute duration of the different building levels of the site Yunatsite, but also show the potential of a dating strategy combining detailed excavations by context and dating of stratified short-lived material. Especially the multilayered tells in the Balkans provide good grounds for modelling approaches using Gaussian Monte Carlo Wiggle Matching and Bayesian statistics.

∴

References

Bayliss A. 2009. Rolling out revolution: Using radiocarbon dating in archaeology. *Radiocarbon 51(1): 123–147.* https://doi.org/10.1017/S0033822200033750

2015. Quality in Bayesian chronological models in archaeology. *World Archaeology 47(4): 677–700.* https://doi.org/10.1080/00438243.2015.1067640

Boyadzhiev J. 1988. A contribution to the problem of the absolute chronology of the eneolithic period in the Balkan Peninsula. *Studia Praehistorica 9: 194–209.*

1995. Chronology of prehistoric cultures in Bulgaria. In D. Bailey, I. Panayotov (eds.), *Prehistoric Bulgaria*. Monographs in World Archaeology 22. Prehistory Press. Madison, Wisconsin: 149-191.

2007. Ploski kostni figurki ot eneolitnata epokha. In M. Stefanovich, C. Angelova (eds.), *PRAE. In Honorem Henrieta Todorova*. Archeologičeski Institut s Muzej. Sofia: 79-94. (in Bulgarian)

2015. Tell Yunatsite: Development and Absolute Chronology of the Settlements from the Beginning of the Chalcolithic to the Early Bronze Age. In S. Hansen, P. Raczky, A. Anders, and A. Reingruber (eds.), *Neolithic and Copper Age between the Carpathians and the Aegean Sea*. Archäologie in Eurasien 31. Habelt. Bonn: 381-394.

Boyadzhiev Y., Aslanis I. 2016. Radiocarbon dates from Tell Yunatsite. In Z. Tsirtsoni (ed.), *The Human Face of Radiocarbon: Reassessing Chronology in prehistoric Greece and Bulgaria, 5000–3000 cal BC*. Maison de l'orient et de la Mediterranée – Jean Pouilloux. Nº 69. Lyon: 157-166.

Boyadzhiev Y. A., Aslanis Ī., and Terziīska-Ignatova S. 2009. Novi danni za ranniya khalkolit v raīona na selish-

tnata mogila Yunatsite. *Izvestiya na Regionalniya istoricheski muzeī Blagoevgrad 5: 105–111.* (in Bulgarian)

Boyadzhiev Y. A., Aslanis Ī., Terziīska-Ignatova S., and Matsanova V. 2004. Selishtna mogila Yunatsite – prouchvaniya prez 2002 g. In *Arkheologiyata – interdistsiplinarni izsledvaniya*. NBU, Departament Arkheologiya 6. Sofiya: 169-174. (in Bulgarian)

2011a. Yunatsite: Ein Bulgarisch-Griechisches Grabungsprojekt. Die Jahre 2002–2008. In Y. Boyadzhiev, S. Terzijska-Ignatova (eds.), *The Golden Fifth Millenium. Thrace and its neighbour areas in the Chalcolithic*. Archeologieški institut s muzej. Sofia: 21-37.

2011b. Selishtna mogila Yunatsite – prouchvaniya prez 2001–2010 g. *Godishnik na Regionalen istoricheski muzeī Pazardzhik 2: 42–55.* (in Bulgarian)

Boyadzhiev Y. A., Boyadzhiev K., and Petrov V. 2015. Selishtna mogila. Yunatsite. *Arkheologicheski otkritiya i razkopki prez 2014 g.* Bŭlgarska akademiia na naukite. Nacionalen Archeologičeski Institut i Muzej. Sofia: 95-98. (in Bulgarian)

2017. Selishtna mogila Yunatsite – khalkoliten plast. *Arkheologicheski otkritiya i razkopki prez 2016 g.* Bŭlgarska akademiia na naukite. Nacionalen Archeologičeski Institut i Muzej. Sofia: 111-113. (in Bulgarian)

Bronk Ramsey Ch., Plicht J. V. D., and Weninger B. 2001. 'Wiggle Matching' Radiocarbon Dates. *Radiocarbon 43 (2A): 381–389.* https://doi.org/10.1017/S0033822200038248

Bronk Ramsey Ch. 2009a. Bayesian Analysis of Radiocarbon Dates. *Radiocarbon 51: 337–360.* https://doi.org/10.1017/S0033822200033865

2009b. Dealing with Outliers and Offsets in Radiocarbon Dating. *Radiocarbon 51: 1023–1045.*
https://doi.org/10.1017/S0033822200034093

Buck C. E., Cavanagh W. G., and Litton C. D. 1996. *The Bayesian approach to interpreting archaeological data.* Wiley. Chicester.

Draşovean F., Schier W., Bayliss A., Gaydarska B., and Whittle A. 2017. The Lives of Houses: Duration, Context, and History at Neolithic Uivar, Romania. *European Journal of Archaeology 20: 636–662.*
doi: 10.1017/eaa.2017.37

Ferguson C. W., Huber B., and Suess H. E. 1966. Determination of the Age of Swiss Lake Dwellings as an Example of Dendrochronologically-Calibrated Radiocarbon Dating. *Zeitschrift für Naturforschung A 21: 1173–1177.*
https://doi.org/10.1515/zna-1966-0745

Görsdorf J., Bojadžiev J. 1996. Zur absoluten Chronologie der bulgarischen Urgeschichte. *Eurasia Antiqua 2: 105–173.*

Görsdorf J., Weninger B. 1992. Berliner ^{14}C-Altersbestimmungen von Datierungsmaterialien aus dem Tell Karanovo. In S. Hiller, V. Nikolov, S. Bökönyi, P. Höglinger, J. Görsdorf, and B. Weninger (eds.), *Tell Karanovo 1992: Vorbericht über die 9. Kampagne der österreichisch-bulgarischen Ausgrabungen am Tell Karanovo: Arbeitsberichte.* Institut für Klassische Archäologie der Universität Salzburg. Salzburg: 20–34.

Hamilton W. D., Krus A. M. 2018. The myths and realities of Bayesian chronological modeling revealed. *American Antiquity 83(2): 187–203.*
https://doi.org//10.101/aq.2017.57

Hinz M., Schmid C., Knitter D., and Tietze C. 2018. oxcAAR: Interface to 'OxCal' Radiocarbon Calibration. R package version 1.0.0. https://CRAN.R-project.org/package=oxcAAR.

Hofmann R. 2013. *Okolište 2 – Spätneolithische Keramik und Siedlungsentwicklung in Zentralbosnien.* Habelt. Bonn.

Horejs B., Weninger B. 2016. Early Troy and its significance for the Early Bronze Age in Western Anatolia. In E. Pernicka, S. Ünlüsoy, and S. W. E. Blum (eds.), *Early Bronze Age Troy: Chronology, Cultural Development and Interregional Contacts.* Habelt. Bonn: 123–145.

Katincharov R., Merpert N. Ya., Titov V. S., Matsanova V. Kh., and Avilova L. I. 1995. *Selishtna mogila pri s. Yunatsite (Pazardzhishko). Istoriya na prouchvaniyata. Obshta stratigrafiya. Plast A. Tom Í.* Agato. Sofiya. (in Bulgarian)

Krauß R., Schmid C., Kirschenheuter D., Abele J., Slavchev V., and Weninger B. 2017. Chronology and development of the Chalcolithic necropolis of Varna I. *Documenta Praehistorica 44: 282–305.*
https://doi.org/10.4312/dp.44.17

Mathieson I., Alpaslan-Roodenberg S., Posth C., +113 authors, and Reich D. 2018. The genomic history of southeastern Europe. *Nature 555: 197–203.*
https://doi.org/10.1038/nature25778

Mazanova V. 1992. Tellsiedlung Junazite – die Spätkupferzeit. *Studia Prahistorica 11–12: 248–261.*

2004. Spätchalkolithische Metallfunde aus Tell Junazite Gebiet Pasardjik. In V. Nikolov, K. Băčvarov, and P. Kalchev (eds.), *Prehistoric Thrace.* Archeologičeski institut s muzej. Sofia-Stara Zagora: 391–401.

2011. Erforschungsgeschichte der Tellsiedlung Yunatzite, Pasardzikregion. In Y. Boyadzhiev, S. Terzijska-Ignatova (eds.), *The Golden Fifth Millenium. Thrace and its Neighbour Areas in the Chalcolithic.* Archeologičeski institut s muzej. Sofia: 9–21.

Matsanova V., Mishina T. 2018. The latest Late Chalcolithic settlement at Tell Yunatsite: Plan and architectural remains. In S. Dietz, F. Mavridis, Z. Tankosić, and T. Takaoğlu (eds.), *Communities in transition. The Circum-Aegean area during the 5th and 4th millennia BC.* Monographs of the Danish Institute at Athens 20. Oxbow books. Oxford and Philadelphia: 128–139.

Meadows J., Müller-Scheeßel N., Cheben I., Agerskov Rose H., and Furholt M. 2009. Temporal dynamics of Linearbandkeramik houses and settlements, and their implications for detecting the environmental impact of early farming. *The Holocene 29(10): 1653–1670.*
https://doi.org/10.1177/0959683619857239

Mikov V. 1940. Selishtna mogila pri s. Yunatsite (Pazardzhishko). *Godishnik na Plovdivskata narodna biblioteka i muzei 1937–1939: 55–84.* (in Bulgarian)

Pearson G. W. 1986. Precise Calendrical Dating of Known Growth-Period Samples Using a 'Curve Fitting' Technique. *Radiocarbon 28(2A): 292–299.*
https://doi.org/10.1017/S0033822200007396

R Core Team 2020. R: A Language and Environment for Statistical Computing. https://www.R-project.org/

Reimer P. J., Austin W. E. N., Bard E., +38 authors, and Talamo S. 2020. The IntCal20 Northern Hemisphere radiocarbon calibration curve (0–55 cal kBP). *Radiocarbon 62: 1–33.* doi:10.1017/RDC.2020.41

Reingruber A., Rassamakin J. 2016. Zwischen Donau und Kuban: Das nordpontische Steppengebiet im 5. Jt. v. Chr. In V. Nikolov, W. Schier (eds.), *Der Schwarzmeerraum von Neolithikum bis in die Früheisenzeit (6000–600 v. Chr.). Kulturelle Interferenzen in der zirkumpontischen Zone und Kontakte mit ihren Nachbargebieten*. Leidorf. Rahden/Westfalen: 273–310.

Reingruber A., Thissen L. online. http://www.14sea.org/3_analysis.html.

Tasić N., Marić M., Filipović D., +6 authors, and Whittle A. 2016. Interwoven Strands for Refining the Chronology of the Neolithic Tell of Vinča-Belo Brdo, Serbia. *Radiocarbon 58: 795–831*. https://doi.org/10.1017/RDC.2016.56

Tell Yunatsite 2007. *Epokha bronzy. Tom ÍÍ. Chast' pervaya*. Vost. lit. Moskva. (in Russian)

Todorova H. 1986. *Kamenno-mednata epokha v Bŭlgariya*. Nauka i izkustvo. Sofiya. (in Bulgarian)

Todorova N. 2003. The ornamentation of Late Chalkolithic pottery from Yunatzite Tell, Pazardzhik district. In L. Nikolova (ed.), *Early Symbolic Systems for Communication in Southeast Europe*. BAR International Series 1139. Archaeopress. Oxford: 291–311.

Todorova N., Mazanova V. 2000. Late Chalcolithic ceramic style at Yunatsite Tell (Approach to the systematization of the ceramics from the newly excavated levels). In L. Nikolova (ed.), *Technology, Style and Society: Contributions to the Innovations between the Alps and the Black Sea in prehistory*. BAR International Series 854. Archaeopress. Oxford: 331–361.

Todorova H., Vaisov I. 2001. *Der kupferzeitliche Schmuck Bulgariens. Prähistorische Bronzefunde*. Abteilung 20. Band 6. Steiner. Stuttgart.

Weninger B. 1986. High-Precision Calibration of Archaeological Radiocarbon Dates. *Acta Interdiscipliniaria Archaeologica 4: 11–53*.

1997. Monte Carlo Wiggle Matching. Zur statistischen Auswertung der mittelneolithischen ^{14}C-Daten von Hasselsweiler 2, Inden 3, und Inden 1. In E. Biermann (ed.), *Großgartach und Oberlauterbach. Interregionale Beziehungen im südwestdeutschen Mittelneolithikum*. Archäologische Berichte 8. Habelt. Bonn: 91– 113.

Weninger B., Jöris O. 2008. A ^{14}C age calibration curve for the last 60 ka: the Greenland-Hulu U/Th timescale and its impact on understanding the Middle to Upper Paleolithic transition in Western Eurasia. *Journal of Human Evolution 55: 772–781*. https://doi.org/10.1016/j.jhevol.2008.08.017

Weninger B., Jung R. 2009. Absolute Chronology of the End of the Aegean Bronze Age. In S. Deger-Jalkotzy, A. E. Bächle (eds.), *LH IIIC Chronology and Synchronisms III: LH IIIC Late and the Transition to the Early Iron Age*. Proceedings of the International Workshop at the Austrian Academy of Sciences at Vienna, February 23rd and 24th, 2007. Verlag der ÖAW. Wien: 373–416.

Appendix

*Tab. 1. List of radiocarbon dates for Tell Yunatsite (*Görsdorf, Boyadzhiev 1996; Boyadzhiev 2015; Boyadzhiev, Aslanis 2016; Mathieson *et al.* 2018*).*

Lab.-No.	BP_Date	cal BC (1σ)	cal BC (2σ)	Material	Building level	Context	Literature
ИГАН-2802	6050±140	5207–4792	5311–4616	charcoal	EC – final	central profile 8.55-8.59m	*Boyadzhiev 2015*
ИГАН-2801	5890±90	4898–4616	4992–4543	charcoal	LC – BIII	central profile 7.08-7.40m	*Boyadzhiev 2015*
ИГАН-2800	5460±170	4455–4054	4696–3955	charcoal	LC – BI	central profile 5.37-5.41m building 12	*Boyadzhiev 2015*
ИГАН-2796	5650±90	4583–4362	4700–4342	decayed wood	LC – BI	central profile 5.30m; building 12	*Boyadzhiev 2015*
ИГАН-2797	5560±70	4455–4341	4545–4258	decayed wood	LC – BI	central profile 5.52m; building 12	*Boyadzhiev 2015*
ИГАН-2793	5410±70	4345–4076	4361–4049	decayed wood	LC – BI	central profile 5.45m; building 12	*Boyadzhiev 2015*
ИГАН-2943	5520±160	4546–4071	4712–3991	bone	LC – BI	skeleton 66	*Boyadzhiev 2015*
ИГАН-2944	5380±130	4341–4052	4493–3952	bone	LC – BI	skeleton 72	*Boyadzhiev 2015*
Ly-14792	5610±40	4488–4365	4536–4354	charcoal	LC – BI	T6 – occupation level close to outer wall	*Boyadzhiev, Aslanis 2016*
Ly-14793	5515±35	4442–4333	4446–4271	big charcoal	LC – BI	F9 – pit next to platform	*Boyadzhiev, Aslanis 2016*
Ly-14794	5725±40	4650–4499	4685–4457	big charcoal	LC – BI	S6–occupation level close to outer wall	*Boyadzhiev, Aslanis 2016*
Ly-5996/ SacA-15565	5630±30	4498–4371	4537–4365	small charcoal	LC – BI	beginning of burnt daub	*Boyadzhiev Aslanis 2016*
Ly-5997/ SacA-15566	5560±30	4443–4355	4451–4346	grains	LC – BI	top part of burnt daub	*Boyadzhiev, Aslanis 2016*
Ly-5998 SacA-15567	5585±35	4448–4364	4493–4348	charcoal	LC – BI	E8 – northern part of the tell	*Boyadzhiev, Aslanis 2016*
Ly-5999 SacA-15568	5560±45	4445–4353	4493–4336	bone and teeth	LC – BI	skeleton 82–on top of burnt daub	*Boyadzhiev, Aslanis 2016*
MAMS-28134	5632±24	4499–4401	4537–4367	bone	LC – BI	skeleton 78–I0781	*Mathieson* et al. 2018
MAMS-28135	5578±23	4446–4363	4451–4354	tooth	LC – BI	skeleton 99–I0785	*Mathieson* et al 2018
Poz-108890	5620±40	4493–4368	4537–4359	animal bone	LC – BII	P5–feature 222–structure B2-21	this study
Poz-109086	5590±40	4451–4362	4498–4347	seeds	LC – BII	O4–feature 385–structure B2-21	this study
Poz-108910	5660±40	4539–4451	4603–4366	animal bone	LC – BII	O7–feature 48–on top of structure B3-1	this study
Poz-109084	5730±40	4654–4501	4688–4458	seeds	LC – BIII	O7–feature 90–structure B3-1	this study
Poz-108885	6130±40	5207–4996	5210–4952	animal bone	LC – BIII	N6–feature 278–under structure B3-1	this study
Poz-108886	5630±40	4500–4369	4541–4361	animal bone	LC – BIV	M7–feature 230–on top of structure B4-2–flotation	this study
Poz-115801	5730±40	4654–4501	4688–4458	animal bone	LC – BIV	M7–feature 225–on top of structure B4-2–flotation	this study
Poz-109419	5460±50	4353–4254	4445–4170	animal bone	LC – BV	M6–feature 35–structure B5-2–poor collagen	this study
Poz-115803	5690±40	4581–4455	4676–4407	animal bone	LC – BVI	M5–feature 118–on top of wooden planks	this study
Poz-108883	5710±40	4606–4463	4678–4453	animal bone	LC – BIV	M3–feature 348–on top structure B5-1	this study
Poz-115802	5700±40	4596–4458	4678–4449	animal bone	LC – BV	L3–feature 396–structure B5-1	this study
Poz-108907	5630±40	4500–4369	4541–4361	animal bone	LC – BVI	M3–feature 439–8.18m	this study
Poz-108905	5680±30	4542–4458	4606–4447	animal bone	LC – BVII	M3–feature 450–9.07m	this study

Lab.-No.	BP_Date	cal BC (1σ)	cal BC (2σ)	Material	Building level	Context	Literature
Poz-108908	5740±40	4676–4538	4700–4461	animal bone	LC – BVIIIa	M3–feature 474–9.45m	this study
Poz-108888	5780±40	4691–4554	4723–4505	animal bone	LC – BVIIIb	M3–feature 484–9.37m	this study
Poz-108906	5810±40	4718–4609	4783–4547	animal bone	LC – BVIIIc	M2–feature 505–9.67m	this study
Poz-108889	5810±40	4718–4609	4783–4547	animal bone	LC – BVIIIc	M2–feature 518–10.4m	this study
Poz-108909	5860±40	4787–4694	4836–4610	animal bone	LC – BVIIId	M3–feature 521–10.4m	this study
Poz-108887	6200±40	5213–5066	5300–5032	animal bone	LC – BVIIId	M2–feature 523–10.32m	this study
ИГАН-2794	4380±70	3259–2904	3333–2889	charcoal	BA – XVII/XVI	central profile – 5.00m	*Boyadzhiev 2015*
ИГАН-2795	4090±60	2851–2501	2872–2476	charcoal	BA – XVII/XVI–XV	central profile – 5.00m	*Boyadzhiev 2015*
Ly-14795	4280±40	2925–2876	3016–2707	grains+chaff	BA – XV	K7–8 – building 34 – 4.64m	*Boyadzhiev, Aslanis 2016*
Bln-3677	4080±70	2852–2495	2873–2471	grains	BA – XV	building 34	*Görsdorf, Boyadzhiev 1996*
Bln-3678	4050±50	2661–2475	2858–2466	grains	BA – XV	building 34	"
Bln-3675	4280±60	3011–2778	3091–2671	grains	BA – XV	building 31	"
Bln-3676	4030±70	2836–2466	2868–2348	grains	BA – XV	building 31	"
Bln-3672	4040±50	2623–2475	2857–2462	charcoal	BA – XIII	building 22	"
Bln-3672A	4040±50	2623–2475	2857–2462	charcoal	BA – XIII	building 22	"
Bln-3671	4180±50	2882–2675	2896–2586	grains	BA – XIII	building 22	"
Bln-3673	3990±60	2620–2357	2842–2296	grains	BA – XIII	building 20	"
Bln-3674	4020±60	2626–2466	2858–2347	grains	BA – XIII	building 20	"
Bln-3670	3990±50	2576–2462	2828–2307	peas	BA – XI	square C 7/C 8 – building 11	"
Bln-3679	4000±70	2629–2352	2857–2294	peas	BA – XI	C 7/C 8 – building 11	"
Bln-3668	3830±60	2435–2151	2466–2066	lentils	BA – X	C 8–building 10	"
Bln-3669	4090±50	2849–2503	2872–2489	grains	BA – X	U 8	"
ИГАН-2799	4070±150	2874–2467	3011–2150	charcoal	BA – X–IX	central profile – 3.30–3.60m	*Boyadzhiev 2015*
Bln-3665	4100±50	2851–2575	2874–2494	wood	BA – IX	P 7	*Görsdorf, Boyadzhiev 1996*
Bln-3666	4070±60	2847–2492	2868–2470	grains	BA – IX	K 8	"
Bln-3667	4050±50	2661–2475	2858–2466	charcoal	BA – IX	L 9	"
ИГАН-2798	4180±250	3283–2352	3508–2047	charcoal	BA – IX–VIII	central profile – 3.30m	*Boyadzhiev 2015*
Bln-3663	4100±50	2851–2575	2874–2494	grains	BA – VIII	O 8/M 6	*Görsdorf, Boyadzhiev 1996*
Bln-3664	4140±50	2866–2631	2879–2579	grains	BA – VIII	O 8/M 6	"
Bln-3662	3910±60	2469–2297	2570–2204	acorns	BA – VII	O 9	"
Bln-3660	3970±50	2573–2354	2621–2298	charcoal	BA – VI	3 9/K 6	"
Bln-3661	4060±60	2840–2476	2868–2467	charcoal	BA – VI	3 9/K 6	"
Bln-3658	3780±50	2292–2136	2434–2034	acorns	BA – V	O 6/O 8	"
Bln-3659	3700±50	2195–1986	2276–1946	acorns	BA – V	O 8/O 9	"
Bln-3657	3760±50	2282–2050	2343–1985	acorns	BA – IV	3 9–1.70m	"
Bln-3656	3760±50	2282–2050	2343–1985	acorns	BA – III	K 6	"

Tab. 2. Context and laboratory information as well as taxonomic determinations on the radiocarbon dates published in this study.

Lab.-No.	BP date	context	square	depth (below site datum)	building level	species	fragment	collagen (%)	N (%)	C (%)	layer description
Poz-108883	5710±40	348	M3		BIV	Ovis/Capra	femur	4.3	2.0	6.5	pile of bones on top greenish clay leveling on top of the oven/building BV-1
Poz-108885	6130±40	278	N6	7,75	BIII	Bos taurus	phalanx	2.4	0.5	3.9	claylayer under destruction of building BIII-1 over the oven – lower layer
Poz-108886	5630±40	230	M7		BIV	n.d.	longbone	1.4	1.5	5.3	clayish layer on top of floor of building BIV-2 – from floatation
Poz-108887	6200±40	523	M2	10,32	BVIIId	Bos taurus	costa	3.9	1.6	8.7	grey ashy layer
Poz-108888	5780±40	484	M3	9,37	BVIIIb	Bos taurus	humerus	3.0	3.4	9.5	grey brown layer with concentration of pottery
Poz-108889	5810±40	518	M2	10,4	BVIIIc	Bos taurus	costa	6.4	3.0	8.9	hard grey clay
Poz-108890	5620±40	222	P5	7,15	BII	Bos taurus	phalanx	3.7	0.9	7.3	building BII-21
Poz-108905	5680±30	450	M3	9,07	BVII	Dama dama	tibia	3.2	2.8	8.2	grey-greenish layer
Poz-108906	5810±40	505	M2	9,67	BVIIIc	Bos taurus	humerus	5.4	3.5	9.6	grey non-homogenous layer - unburned wooden planks
Poz-108907	5630±40	439	M3	8,18	BVI	Ovis/Capra	metacarpus	3.1	2.8	8.2	floor level
Poz-108908	5740±40	474	M3	9,45	BVIIIa	Bos taurus	costa	5.7	3.9	9.8	grey ashy layer
Poz-108909	5860±40	521	M3	10,4	BVIIId	Bos taurus	metacarpus	2.7	4.0	11.0	grey layer with some charcoals
Poz-108910	5660±40	48	O7		BII	Bos taurus	phalanx	2.1	7.6	19.7	Phase 2 on top of building BIII-1 – homogeneous layer of clay surfaces
Poz-109084	5730±40	90	O7	7,21	BIII	grains					concentration of grains in burnt destruction of building B3-1
Poz-109086	5590±40	385	O4	7,53	BII	lentils					Burnt destruction of building B2-21 (in pot 10 under feature 385)
Poz-109419	5460±50	35	M6		BV	Bos taurus	phalanx	0.2	1.6	5.8	destruction of building BV-2 – low collagen
Poz-115801	5730±40	225	M7		BIV	Ovis/Capra	vertebra	2.8	2.6	8.9	clayish layer on top of floor of building BIV-2 – from floatation
Poz-115802	5700±40	396	L3		BV	Bos taurus	phalanx	1.2	0.7	4.4	lower floor level of building BV-1
Poz-115803	5690±40	118	M5	8,15	BVI	ungulate	vertebra	1.0	1.2	5.4	claylayer on top of unburned wooden planks